SUPPLEMENTAL EXPERIMENTAL PROCEDURES

Flow Cytometry Analysis, phospho-flow analysis and Sorting

For the phenotypical characterization of HP, LDBM cells were obtained after separation using Histopaque-1083 (Sigma, Saint Louis, MO) and stained with fluorescein isothiocyanate (FITC)-conjugated lineage markers CD45R (B220; clone RA3-6B2), Gr-1 (Ly-6G and Ly-6C; clone RB6-8C5), CD4 (L3T4; clone RM4-5), CD8a (Ly-2; clone 53-6.7), CD3e (clone 145-2C11), CD11b (M1/70), and Ter119 (Ly-76), allophycocyanin (APC)-conjugated c-Kit and phycoerythrin (PE)-PerCP cy5.5-conjugated Sca-1 antibodies to identify the $Lin^-/c\text{-}kit^+/Sca\text{-}1^+$(LSK) BM cell population. IL7Rα (PE Cy7 conjugated, clone SB/199), CD34 (Pacific blue, clone RAM34), CD16/CD32 (PE conjugated, clone 2.4G2) were used for further characterization. Long-term HSC (LT-HSC), ST-HSC and multipotent progenitors (MPP) were identified as follows: $IL7R\alpha^-$ Lin^-,$Sca1^+c\text{-}kit^+$(LSK) $CD34^-Flk2^-CD150^+$ and $IL7R\alpha^-$ Lin^-,$Sca1^+c$-kit+(LSK) $CD34^+Flk2^-$ and Lin^-,$Sca1^+c\text{-}kit^+$(LSK) $CD34^+Flk2^+$ respectively. Myeloid and lymphoid progenitors were identified as follows: $IL7R\alpha^-$ $Lin^-Sca1^-c\text{-}kit^+CD34^+FcγRII/III^{lo}$ (common myeloid progenitors, CMP), $IL7R\alpha^-Lin^-Sca1^-c\text{-}kit^+CD34^+FcγRII/III^{hi}$ (granulocyte-monocyte progenitors, GMP), or $IL7R\alpha^-$ $Lin^-Sca1^-c\text{-}kit^+CD34^-FcγRII/III^{lo}$ (megakaryocyte-erythroid progenitors, MEP) or $IL\text{-}7R\alpha^+Lin^-Sca1^{lo}c\text{-}kit^{lo}$ (common lymphoid progenitors, CLP). B lymphoid cell populations were distinguished as $B220^+/CD19^-$(pre-pro B), $B220^+/CD19^+/CD43^+$ (pro B), $B220^+/CD19^+/CD43^-$ IgM^- (pre B), $B220^+/CD19^+/CD43^-/IgM^+/IgD^-$ (immature B) and $B220^+/CD19^+/CD43^-/IgM^+/IgD^+$ (mature B). For the analysis of FAK and pFAK, Obs were fixed with pre-cold 4% paraformaldehyde for 10 minutes on ice then permeabilized with cytofix/cytoperm solution according to manufacturer's instructions (BD). Primary antibodies against FAK (abcam, clone 63D5) and pFAK (phospho Y397, abcam) were incubatedwith 1:100 dilution for 1h at room temperature. Mouse IgG1 and rabbit IgG were used as isotype controls. Goat anti-mouse Alexa fluor 568 and goat anti-rabbit Alexa fluor 633 were used at 1:2,000 dilutions for the secondary

antibody staining. All types of cells were analyzed or sorted by flow cytometry (FACS Canto and FACSAria II, BD Biosciences, San Jose, CA).

Cell cycle analysis

For cell cycle analysis, we used FACS analysis using bromodeoxyuridine (BrdU) incorporation along with DNA binding of 7-aminoacinomycin D (7-AAD). One mg of BrdU solution in PBS was injected intraperitoneally into each mouse. Mice were sacrificed and femora were harvested 1 hour post-BrdU injection. Cell suspensions were stained,fixed and permeabilized as per manufacturer's protocol with anti-BrdU-APC (BD Pharmigen, San Jose, CA). For total DNA binding 20 μg/mL 7-AAD was added before FACS analysis and cell cycle phases (G0/G1, S, and G2/M) were distinguished based on BrdU and 7-AAD staining in dot plots using conventional methods of doublet discrimination and light scatter properties.

Micro Computerized Tomography (Micro-CT) analysis

The femora from chimeric Wt HM or p62-/- HM mice were harvested and stored in formalin solution. Mouse femora were scanned using a micro-CT scanner (MicroCAT II, Siemens Preclinical Solutions, Knoxville, TN) at the highest resolution mode; Number of projections: 570, X-ray tube voltage: 80 kV, X-ray tube current: 150 microAmps; Exposure time: 8.96 seconds per projection. To monitor and ensure the image signal intensities were stable for the scans, four rods having varying X-ray attenuation characteristics were placed in the image field-of-view. Micro-CT data sets were reconstructed using a cone beam reconstruction algorithm, COBRA 6.9.42 (Exxim Computing Corporation, Pleasanton, CA) and imported into image analysis software (MicroView 2.1.2, GE Healthcare, Barrington, IL) for quantitative analysis of the trabecular structure in the distal femur. The reconstructed data set size was 1536 x 1536 x 1024 and the reconstructed voxel size was 9.7 μm isotropic. The region-of-interest (ROI) used for analysis of the femur trabecular structure was a cylinder centered in the distal femur. The ROI

started at a level proximal to the condyles and continued for 300 slices towards the femoral head (i.e. proximally). The ROI cylinder was centered in the marrow space and excluded any cortical bone.

5-fluorouracil (5-FU) administration

Mice were administered with 5-FU (APP Pharmaceuticals, Inc., Schaumburg, IL) intravenously (150 mg/kg, single dose) and bled on the indicated days. PB samples were collected by retro-orbital bleeding. An automated total cell count (Drew Scientific Inc., Oxford, CT) was performed.

Isolation and differentiation of Obs

Calvaria from newborn or 2 day-old mice were dissected under sterile conditions. After removal of periosteum and endosteum, two to six calvaria of each genotype group were cut into small pieces (1–2 mm), pooled, and digested in a solution containing 2 mg/mL of collagenase A (Roche) in serum-free medium at 37°C for 10minutes. The medium was discarded and replaced with fresh collagenase-containing medium plus a solution of DNase (5 μg/mL). After 2 hours digestion at 37°C, bone debris was separated by using a 70-μm nylon mesh (BD Falcon). Cells were washed by centrifugation several times to remove excess collagenase and DNase enzymes, resuspended in α-MEM supplemented with 10% FCS, and plated at 2×10^4 cells/cm^2. All the experiments were performed using cells from the first 2-3 passages.

Preparation of BM-derived MΦ

RBC lysed BMNC were isolated from Ubiquitin-EGFP mouse then plates in T25 flask with DMEM supplemented with 10 % FCS and 50 ng/ml M-CSF (PeproTech, Rocky Hill, NJ). The next day, non-adherent cells were collected and transferred to T75 flask and then cultured in the presence of 100 ng/mL M-CSF for one week. To characterize the expanded population, Alexa

fluor conjugated-anti CD68 (BioLegend, clone FA-11), efluor 450 conjugated-anti F4/80 (eBioscience, clone BM8),PE conjugated-anti CD169 (BioLegend, clone 3D6.112), and PerCP-efluor 710 conjugated-anti CD115 (eBioscience, clone AFS98) antibodies were used for flow cytometry analysis.

Cocultures of Ob and BM-derived MΦ

All coculture experiments were performed for a period of 24 hours in a medium containing DMEM, 10% fetal calf serum, 50 IU/mL penicillin and 0.1 mg/mL streptomycin.

Depletion of MΦ in vivo

The clodronate and vehicle containing liposomes were purchased from Clodronateliposomes (Haarlem, The Netherlands).Two hundred µl (PBS-liposomes or clodronate-liposomes) per mouse was administered intraperitoneally once. The PB from the mice was analyzed 2 days post liposome injection using FACS analysis and CFU-C assays.

Detection of cytokines using Luminex or Elisa

The level of cytokines from BM or plasma were determined by enzyme-linked immunosorbent assay (ELISA) or by using multi-analyte profiling beads using MilliplexTM Multiplex kits (Millipore, Billerica, MA) according to manufacturer's instructions. Concentrations of cytokines and chemokines were calculated from standard curves using recombinant proteins. The concentration of Ccl4 from cell culture supernatants was measured according to manufacturer's protocol (R&D Systems).

Chemotaxis assay

Bottom wells of 24-well transwell plate (Corning Inc., Lowell, MA) containing pre-formed cocultures of Wt MΦ and WT or p62-/- Ob in a 1:1 ratio, as described in Material and Methods

and used in all co-culture experiments were used. Recombinant Cxcl12 (100 ng/mL; R&D Systems, Inc., Minneapolis, MN) in presence of anti-Ccl4 antibody (1 μg/ml; R&D Systems, Inc.), BAY 11-7085 (1 μM; Santa Cruz) or Bafilomycin A1 (0.01 μM; Santa Cruz) wereadded to the bottom wells and a gradient of Cxcl12 was allowed to be established for 30 minutes of incubation at 37°C, 5% CO_2 towards the upper transwell chambers. Controls included pre-immune goat IgG (1 μg/mL, R&D Systems, Inc.) or 0.01% DMSO. Wt HP responses to chemotaxis gradients of Cxcl12 in presence of cellular cocultures and aforementioned chemicals and antibodies were analyzed by adding 5×10^4 Wt LDBM cells onto the top chamber and incubation at 37°C, 5% CO_2. After 4 hours, cells in suspension and adhered to the bottom chamber were collected by tripsinization and the number of migrating hematopoietic progenitors was determined by a CFU-C assay. The progenitor migration was determined dividing the number of colonies present in the output fraction by the number of input CFU-C and multiplied by 100 and presented as a percentage. All assays were performed in triplicate in a minimum of two independent experiments.

Viral Transduction

Wt or $p62^{-/-}$ Ob were transduced with MSCV-IRES-eGFP bicistronic retroviral vector encoding full length of p62 or Δ69-71A mutant of p62 in the presence of the recombinant fragment of fibronectin, CH296 (Takara Bio Inc) for 16 hours at 37°C. The empty vector, MIEG3, was used as a transduction control for stable expression in Ob.

Quantification of DNA bound active NF-κB p65 and inhibition of NF-κB activity

DNA bound total NF-κB p65 was calculated from freshly isolated nuclear fraction of cultured cells according to manufacturer's protocol (Invitrogen). To block NF-κB activation and phoshphorylation of IκBα, 1μM BAY 11-7085 (Santa Cruz) were added to the cell culture. 0.001% DMSO was used as a vehicle control.

Immunofluorescence and confocal microscopy imaging

The paraffin embedded femurs from the chimeric Wt HM or p62-/- HM mice were cut by longitudinal sections with 4-μm thickness. De-paraffinized bone sections or in vitro-cocultured Ob with MΦ were fixed with 4% paraformaldehyde, permeabilized with 0.1% Triton X-100 for 10 min and blocked with 5% normal mouse serum for 30 minutes. Slides were stained with primary antibodies; anti-NF-κB p65(Santa Cruz, clonec-20), anti- Col1a1 (Santa Cruz, cloneD-13), anti-Ccl4 (R&D, BAF451), anti-LAMP2 (abcam, clone GL2A7) at 4°C overnight and counterstained with secondary antibodies; goat anti-rabbit Alexa fluor 633, goat anti-rabbit Alexa fluor 488, goat anti-rat Alexafluor 568, donkey anti-goat Alexafluor 568 or Alexafluor 568 conjugated- streptavidin (all from Invitrogen) at 1:500 v/v concentration for 1h at room temperature. The stained cells were analyzed by a LSM 510 confocal system (Carl Zeiss) equipped with an inverted microscope (Observer Z1, Carl Zeiss) using a Plan Apochromat 63X 1.4 NA oil immersion lens and processed using Adobe Photoshop v7. TRAP assay of longitudinal 4μm-femoral sections was performed according to manufacturer's instructions (Sigma-Aldrich).

Immunoblot analysis

Protein extracts were prepared using a radioimmunoprecipitation lysis buffer (RIPA, Cell Signaling Technology, Danvers, MA) supplemented with protease and phosphatases inhibitor cocktails (Roche Applied Science, Mannheim, Germany). The lysates were separated using 10% SDS-PAGE gels, transferred to PVDF membranes and detected with antibodies. The primary antibodies used were directed against β-actin (Sigma Aldrich, clone AC-15), p62 (BD, clone 3/p62), IκBα (clone 44D4, Cell Signaling), phospho-IκBα (Ser32/36, clone 5A5, Cell Signaling), NF-κB p65 (clone L8F6, Cell Signaling), IκKα(clone 3G12, Cell Signaling),

IκKβ(clone L570, Cell Signaling) and IκKγ (clone DA 10-12, Cell Signaling). Gels were visualized using autoradiography and band density analyzed (Image J software, National Institutes of Health, USA) at the expected electrophoretic moiety for each protein molecular weight.

Quantitative RT-PCR analysis

Total mRNA from FACS sorted Ob or MΦ was isolated using Qiagen RNAse micro Kit according to the manufacturer's protocol. The mRNA was transcribed using an oligo(dT) primer with Superscript reverse transcriptase (Invitrogen) and amplified cDNA (Taqman Universal 2X Mater Mix , Applied Biosystems,Foster City, CA) were measured by quantitative real-time PCR using the ABI 7500 Sequence Detection System (Applied Biosystems). Cycle threshold (Ct) values of individual genes were normalized to the Ct values of GAPDH to calculate ΔCt and relative gene expression ($2^{-\Delta\Delta Ct}$).

Statistical analysis

Quantitative data is given as mean ± standard error of the mean (SEM). Statistical significance was determined using an unpaired Student-t test, one-way or two-way Anova with Bonferroni correction. A value of $p< 0.05$ was considered to be statistically significant.

SUPPLEMENTAL FIGURE LEGENDS

Figure S1. Loss of p62 does not affect the levels of circulating medium- and long-term HSC or induce cell-autonomous HSC/P loss of activity. Related to Figure 1. (A) Count of circulating LT-HSC ($Lin^-/c\text{-}kit^+/Sca\text{-}1^+/CD34^-/CD135^-$) in PB from Wt and $p62^{-/-}$ mice from mice in Fig. 1A. (B-C) Normalized medium (10-week)- and long (16 weeks) term chimera of Wt and $p62^{-/-}$ mice from experiment described in Fig. 1B (p=N.S.). (D-E) Counts of common lymphoid progenitor (D) and B-lymphoid cell populations in peripheral blood (E) immunophenotypically defined as described in Supplementary Material and Methods and in Fig. 1A, of Wt (grey bars) and p62-deficient mice (black bars). (F) Schema of competitive transplantation to generate primary and secondary chimeric mice. BM cells from $CD45.2^+$ Wt or $p62^{-/-}$ mice were mixed with $CD45.1^+$ $B6.SJL^{Ptprca\ Pep3b/BoyJ}$ wild type BM cells and competitively transplanted into lethally irradiated $CD45.1^+$ $B6.SJL^{Ptprca\ Pep3b/BoyJ}$ primary and secondary recipient mice. $CD45.2^+$ chimera was monitored at different time points. (G-H) Evolution of $CD45.2^+$ chimera in PB of primary recipient mice (G, n=6-8 mice per group) and secondary recipient mice (H, n=5-8 mice per group). Data are presented as mean ± SD. (I-K) Femoral content of BM myeloid progenitors (CFU-C) (I), CLP (J) and B-cell populations in Wt and $p62^{-/-}$ mice. N≥5 mice per group. (L-M) Evolution of absolute neutrophil (L) and platelet (M) counts in the PB of Wt or $p62^{-/-}$ mice after 5-FU administration. N=6-8 mice per group. Data are presented as mean ± SD.

Figure S2. p62 deficiency does not impair the proliferation of HSC or myeloid progenitors. Related to Figure 1. (A) Schema of non-competitive transplantation to generate hematopoietic $p62^{-/-}$ mice (H-$p62^{-/-}$) and H-Wt controls. BM cells from $CD45.2^+$ Wt or $p62^{-/-}$ mice were transplanted into lethally irradiated $CD45.1^+$ $B6.SJL^{Ptprca\ Pep3b/BoyJ}$ wild type mice. (B) Frequency of hematopoietic progenitors in PB of recipient mice (n=8 mice per group) after 6 weeks of transplantation. (C-E) Cell cycle analysis of LT-HSC (C), ST-HSC (D) and LK (E) BM

cells in primary Wt and p62$^{-/-}$ mice. (F-H) Cell cycle analysis of LT-HSC (F), ST-HSC (G) and LK (H) BM cells in Wt HM and p62$^{-/-}$ HM mice generated as described in Fig. 1E. N≥4 mice per group. Values represent mean ± SD. p=N.S. (I-K) Homing of Wt BM ST-HSC (I) and LSK cells (J) and LK cells (K) into myeloablated BM of Wt or p62$^{-/-}$ mice. N=5-8 mice per group in a minimum of two independent experiments. Values represent mean ± SEM. p=N.S.

Figure S3. BM derived MΦ contact with Obs and signal through FAK and NF-kB but not Erk or p38 MAPK and p62-deficient osteoclasts are indispensable. Related to Figures 2 and 3. (A) MΦ can be found in close proximity to endosteal Obs in vivo. F4/80 (green), Collagen I (ColI, red) and DAPI counterstain (blue) in longitudinal femoral sections of Wt HM and p62$^{-/-}$ HM mice. (B) Fraction of high magnification fields where MΦ (F4/80+, green) and Ob (ColI+) were found in either trabecular or endosteal bone. A minimum of 12 high magnification (scale bar= 20μm) fields were analyzed per bone. A minimum of three femora from different chimeric mice were analyzed per group. (C) Representative examples of TRAP staining of longitudinal sections of femurs from Coll1α-Cre;Wt and Coll1α-Cre; p62$^{f/f}$ femora, from Fig. 2J. (D) TRAP positive osteoclasts per field. A minimum of 17 fields were analyzed. Scale bar = 100μm. (E) BMNC from ubiquitin C-EGFP mice were cultured for 7 days with 100ng/ml M-CSF then phenotypically characterized by flow cytometry. (F) Activation of Ob FAK measured by phospho-flow analysis. The pFAK/FAK levels of Wt or p62 deficient Ob alone (solid bars) were compared to the levels of pFAK in Ob cultured for 24 hours with Wt EGFP^{+} MΦ (mosaic bars). N=3 independent cultures per group done by duplicate. **p<0.005; *** p<0.001. (G) Representative immunoblots of phosphorylated ERK and phosphorylated p38 expression in Wt or p62 deficient Ob with or without 24 hours contact of wild type MΦ. β-actin was used as a loading control. (H) Frequency of hematopoietic progenitors in PB of Wt or p62$^{-/-}$Erk1$^{-/-}$ mice (n=6 mice per group). Values represent mean ± SEM. *p<0.05. (I-J) NF-κB p65 in nucleus from flow cytometry sorted Wt or p62$^{-/-}$ Ob (I) or MΦ (J) after 24 hours co-culture with wild type MΦ. 1 μM BAY 11-7085

(hatched bars) treated cells were compared to vehicle control (DMSO, solid bars) treated cells as in Figs. 3H-J. Values represent mean ± SEM. *p<0.05, **p<0.005, *** p<0.001.

Figure S4. Quantification of relevant chemokines and cytokines in plasma and extracellular femoral fluid of Wt HM and p62$^{-/-}$ HM mice. Related to Figure 4. Plasma concentrations of Ccl4 (A), Il-1α (B), Il-1β (C), Tnf-α (D), Ifn-γ (E), Il-10 (F), and G-csf (G) from Wt HM or p62$^{-/-}$ HM mice were detected and measured by luminex assay. Rnkl (H), Osteoprotegerenin (I), Osteocalcein (J), Leptin (K), Ccl3 (L), RANTES (M), and Vegf (N) in BM from Wt HM or p62$^{-/-}$ HM mice were also measured by luminex assay similarly to Fig. 4A. Values represent mean ± SEM with a minimum of 3 mice per group.

Figure S5. Cxcl12 levels are not reduced in plasma or bone of HM p62$^{-/-}$ mice, however, in vivo depletion of MΦ induces hypermigration to the level of HM p62$^{-/-}$ mice. Related to Figure 4. Plasma (A) and femoral (B) levels of Cxcl12 were determined by Elisa in specimens from Fig. 4A. * p<0.05. N≥4 mice per group. (C) Representative FACS dot plots to confirm the depletion of subsets of MΦ in vivo after clodronate-liposome administration. (D) Circulating CFU-C content in peripheral blood before or after injection of clodronate containing liposomes. Vehicle (PBS) containing liposomes were administered as control. N≥8 mice per group. Values represent mean ± SEM. *p<0.05;**p<0.01.

Figure S6. Ectopic expression of p62 and p62 mutant in p62$^{-/-}$ Ob and relation to IKK/NF-κB and Ccl4 expression or activity. Related to Figures 5 and 6. (A) Representative immunoblot of p62 expression in mock vector transduced Wt (Wt + Mock) or p62 deficient Ob (p62$^{-/-}$ + Mock) or full length of p62 transduced-p62 deficient Ob (p62$^{-/-}$ + p62) analyzed in Figs. 5A-E. Retroviral transduced cells were sorted by flow cytometry as a population of EGFP^{+}. β-actin was used as a loading control. (B) Representative confocal microscopic images of NF-κB

p65 (red) and nuclear (DAPI, blue) in retroviral-transduced (EGFP) Wt or $p62^{-/-}$ Ob. TNFα (10 ng/mL) was added to culture media of Ob for positive control of NF-κB p65 nuclear translocation. Data are representative of two independent experiments with similar results. (C) Representative immunoblots of IKK catalytic subunits α, β or γ cytosolic expression in in mock vector transduced Wt (Wt + Mock) or p62 deficient Ob ($p62^{-/-}$ + Mock) or full length of p62 transduced- p62 deficient Ob ($p62^{-/-}$ + p62) after 24 hours contact of wild type MΦ. β-actin was used as a loading control. (D) Representative immunoblot of P62 expression in mock vector transduced p62 deficient Ob (Mock) or Δ69-72A mutant of p62 transduced-p62 deficient Ob (Δ69-72A) used in Figs. 6A-C. Retroviral transduced cells were sorted by flow cytometry as a population of $EGFP^{+}$. β-actin was used as a loading control. (E) Proposed model of interplay between MΦ, Ob and HSC/P. Contacting MΦ induces NF-κB activation in Ob. Activation of FAK, IKK and NF-κB in Ob is induced by macrophages resulting in inhibition of Ob differentiation and Ccl4 expression. NF-κB signaling intermediate levels are controlled by p62-dependent mechanisms of autophagic degradation and in absence of p62, osteogenesis and Ccl4 production are decreased in vitro and in vivo, resulting in loss of BM HSC/P retention.

Figure S1

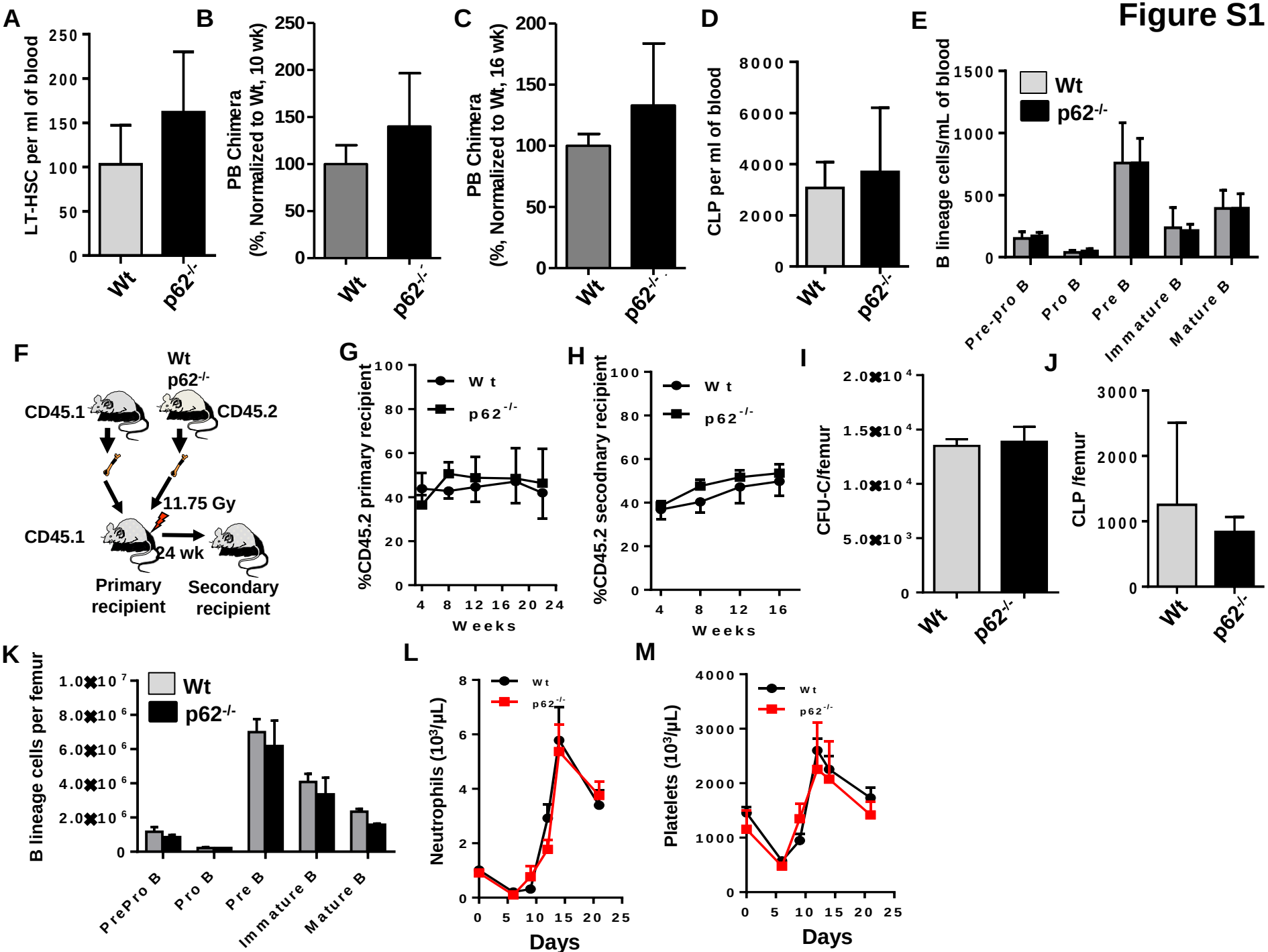
A
LT-HSC per ml of blood
250
200
150
100
50
0
Wt
p62-/-
B
PB Chimera
(%, Normalized to Wt, 10 wk)
250
200
150
100
50
0
Wt
p62-/-
C
PB Chimera
(%, Normalized to Wt, 16 wk)
200
150
100
50
0
Wt
p62-/-
D
CLP per ml of blood
8000
6000
4000
2000
0
Wt
p62-/-
E
B lineage cells/mL of blood
1500
1000
500
0
Wt
p62-/-
Pre-pro B
Pro B
Pre B
Immature B
Mature B
F
Wt
p62-/-
CD45.1
CD45.2
11.75 Gy
CD45.1
24 wk
Primary recipient
Secondary recipient
G
%CD45.2 primary recipient
100
80
60
40
20
0
Wt
p62-/-
4 8 12 16 20 24
Weeks
H
%CD45.2 secodnary recipient
100
80
60
40
20
0
Wt
p62-/-
4 8 12 16
Weeks
I
CFU-C/femur
2.0x10 4
1.5x10 4
1.0x10 4
5.0x10 3
0
Wt
p62-/-
J
CLP /femur
3000
2000
1000
0
Wt
p62-/-
K
B lineage cells per femur
1.0x10 7
8.0x10 6
6.0x10 6
4.0x10 6
2.0x10 6
0
Wt
p62-/-
PrePro B
Pro B
Pre B
Immature B
Mature B
L
Neutrophils (10³/μL)
8
6
4
2
0
Wt
p62-/-
0 5 10 15 20 25
Days
M
Platelets (10³/μL)
4000
3000
2000
1000
0
Wt
p62-/-
0 5 10 15 20 25
Days

Figure S2

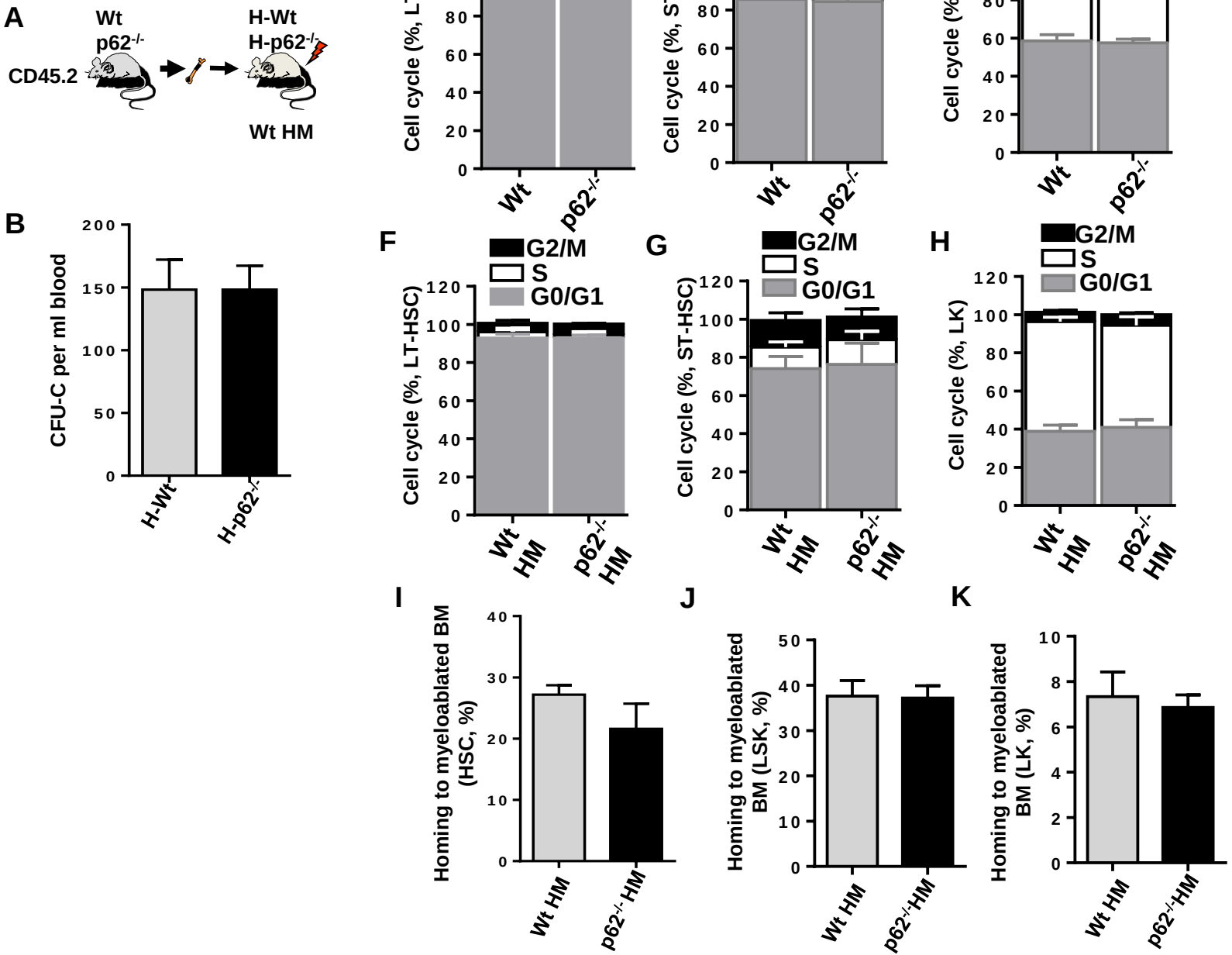
A
Wt
p62-/-
CD45.2
H-Wt
H-p62-/-
Wt HM
B
CFU-C per ml blood
H-Wt
H-p62-/-
C
G2/M
S
G0/G1
Cell cycle (%, LT-HSC)
Wt
p62-/-
D
Cell cycle (%, ST-HSC)
E
Cell cycle (%, LK)
F
Wt HM
p62-/- HM
G
H
I
Homing to myeloablated BM (HSC, %)
J
Homing to myeloablated BM (LSK, %)
K
Homing to myeloablated BM (LK, %)

Figure S3

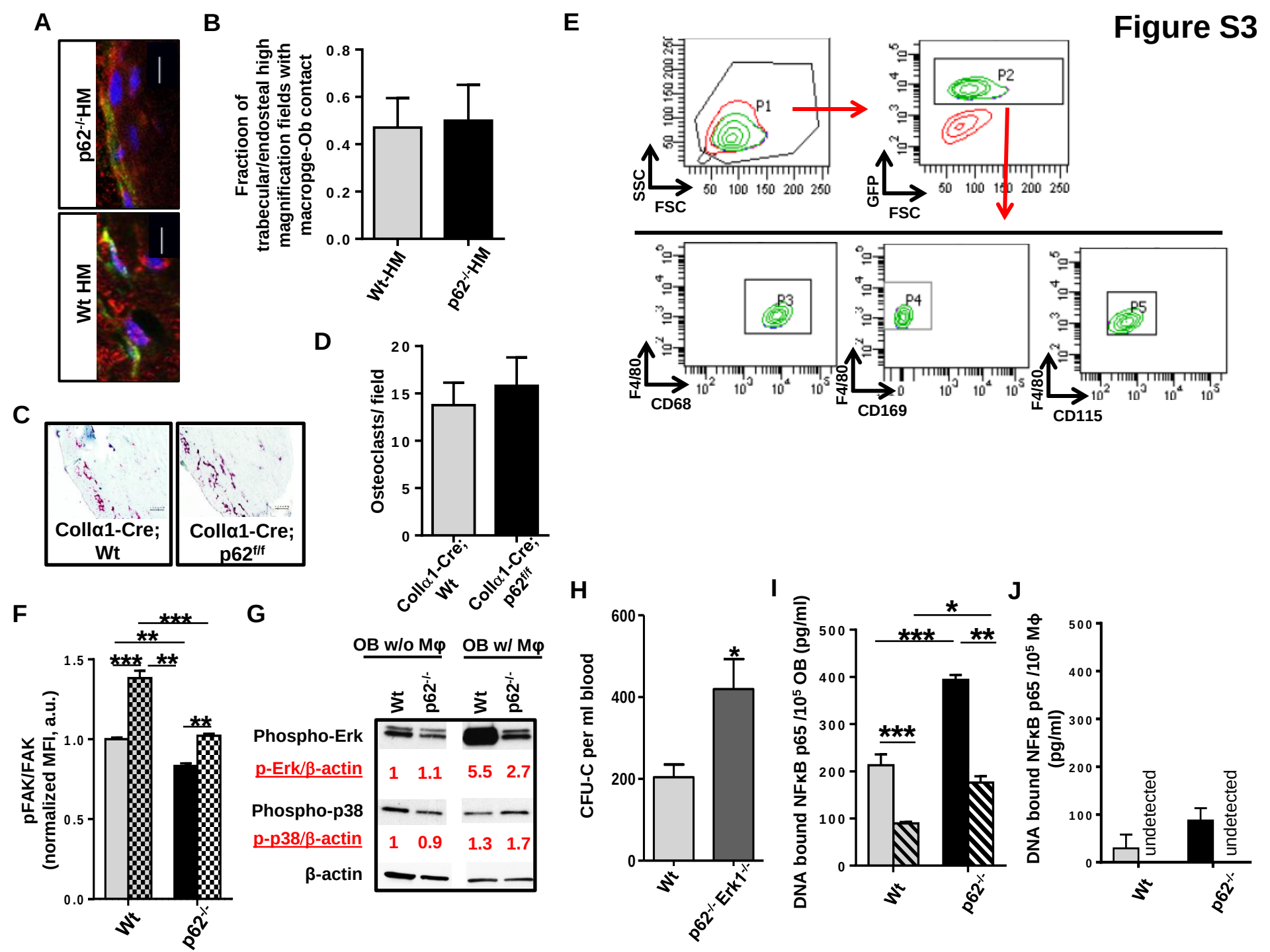
A
p62-/-HM
Wt HM
B
Fractioon of trabecular/endosteal high magnification fields with macropge-Ob contact
0.8
0.6
0.4
0.2
0.0
Wt-HM
p62-/-HM
C
Collα1-Cre; Wt
Collα1-Cre; p62f/f
D
Osteoclasts/ field
20
15
10
5
0
Collα1-Cre; Wt
Collα1-Cre; p62f/f
E
P1
SSC
FSC
P2
GFP
FSC
P3
F4/80
CD68
P4
F4/80
CD169
P5
F4/80
CD115
F
pFAK/FAK (normalized MFI, a.u.)
1.5
1.0
0.5
0.0
***
**
***
**
**
Wt
p62-/-
G
OB w/o Mφ
OB w/ Mφ
Wt
p62-/-
Wt
p62-/-
Phospho-Erk
p-Erk/β-actin
1
1.1
5.5
2.7
Phospho-p38
p-p38/β-actin
1
0.9
1.3
1.7
β-actin
H
CFU-C per ml blood
600
400
200
0
*
Wt
p62-/- Erk1-/-
I
DNA bound NFκB p65 /10^5 OB (pg/ml)
500
400
300
200
100
0
*
***
**
***
Wt
p62-/-
J
DNA bound NFκB p65 /10^5 Mφ (pg/ml)
500
400
300
200
100
0
undetected
undetected
Wt
p62-/-

Figure S4

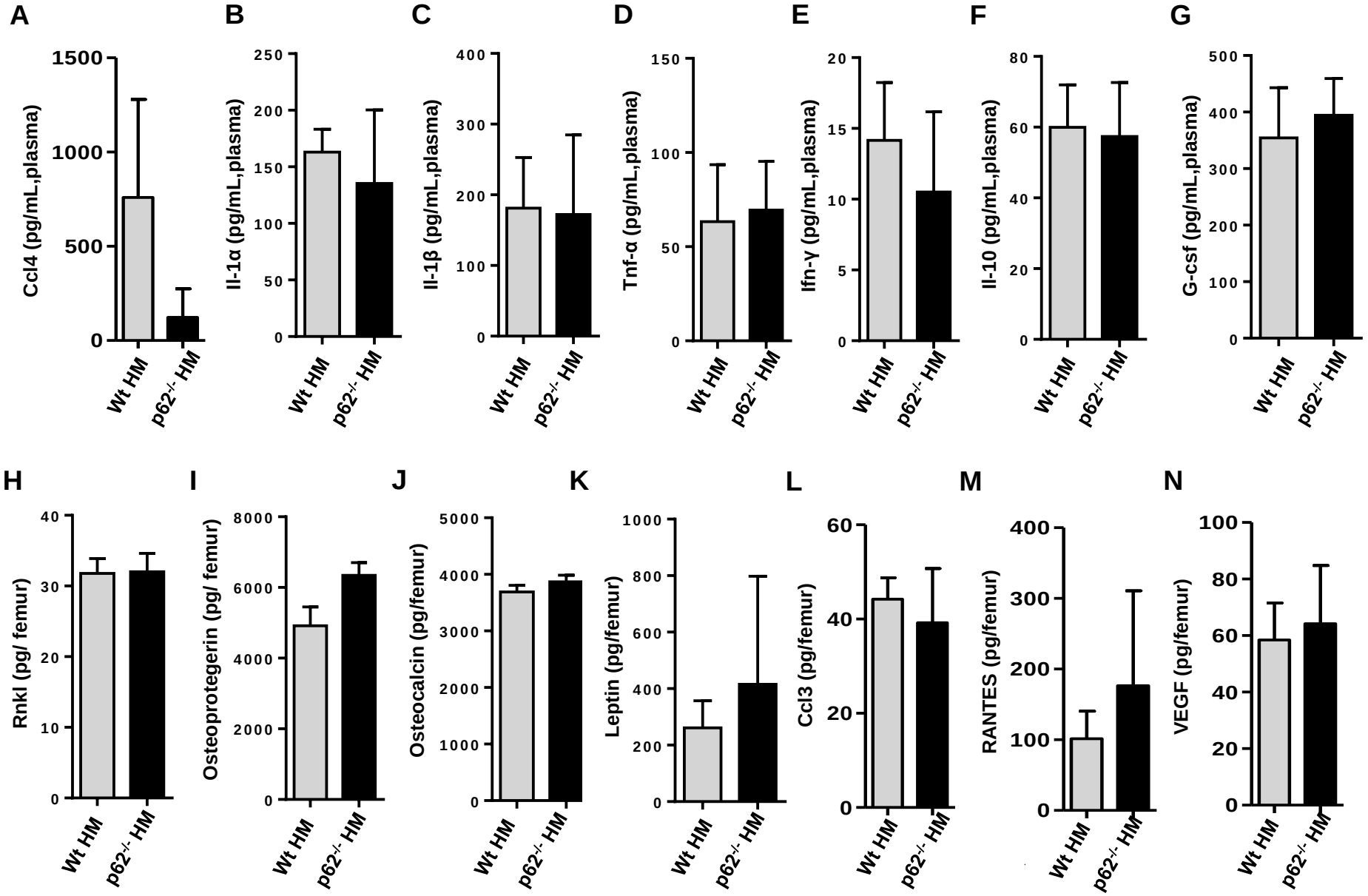
A
Ccl4 (pg/mL,plasma)
1500
1000
500
0
Wt HM
p62-/- HM
B
Il-1α (pg/mL,plasma)
250
200
150
100
50
0
Wt HM
p62-/- HM
C
Il-1β (pg/mL,plasma)
400
300
200
100
0
Wt HM
p62-/- HM
D
Tnf-α (pg/mL,plasma)
150
100
50
0
Wt HM
p62-/- HM
E
Ifn-γ (pg/mL,plasma)
20
15
10
5
0
Wt HM
p62-/- HM
F
Il-10 (pg/mL,plasma)
80
60
40
20
0
Wt HM
p62-/- HM
G
G-csf (pg/mL,plasma)
500
400
300
200
100
0
Wt HM
p62-/- HM
H
Rnkl (pg/ femur)
40
30
20
10
0
Wt HM
p62-/- HM
I
Osteoprotegerin (pg/ femur)
8000
6000
4000
2000
0
Wt HM
p62-/- HM
J
Osteocalcin (pg/femur)
5000
4000
3000
2000
1000
0
Wt HM
p62-/- HM
K
Leptin (pg/femur)
1000
800
600
400
200
0
Wt HM
p62-/- HM
L
Ccl3 (pg/femur)
60
40
20
0
Wt HM
p62-/- HM
M
RANTES (pg/femur)
400
300
200
100
0
Wt HM
p62-/- HM
N
VEGF (pg/femur)
100
80
60
40
20
0
Wt HM
p62-/- HM

Figure S5

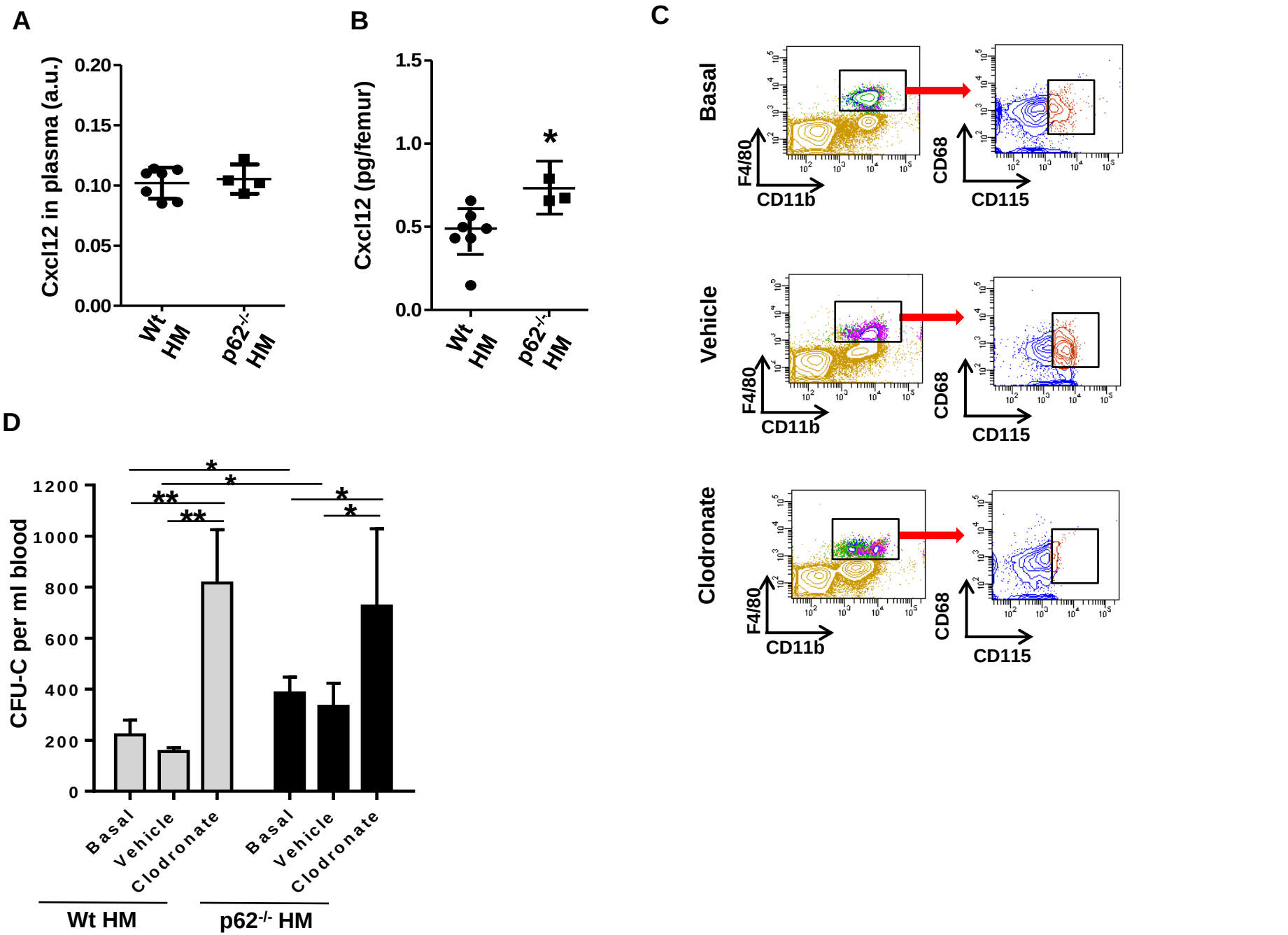
A
Cxcl12 in plasma (a.u.)
0.20
0.15
0.10
0.05
0.00
Wt HM
p62-/- HM
B
Cxcl12 (pg/femur)
1.5
1.0
0.5
0.0
*
Wt HM
p62-/- HM
C
Basal
Vehicle
Clodronate
F4/80
CD11b
CD68
CD115
D
CFU-C per ml blood
1200
1000
800
600
400
200
0
*
*
**
**
*
*
Basal
Vehicle
Clodronate
Basal
Vehicle
Clodronate
Wt HM
p62-/- HM

Figure S6

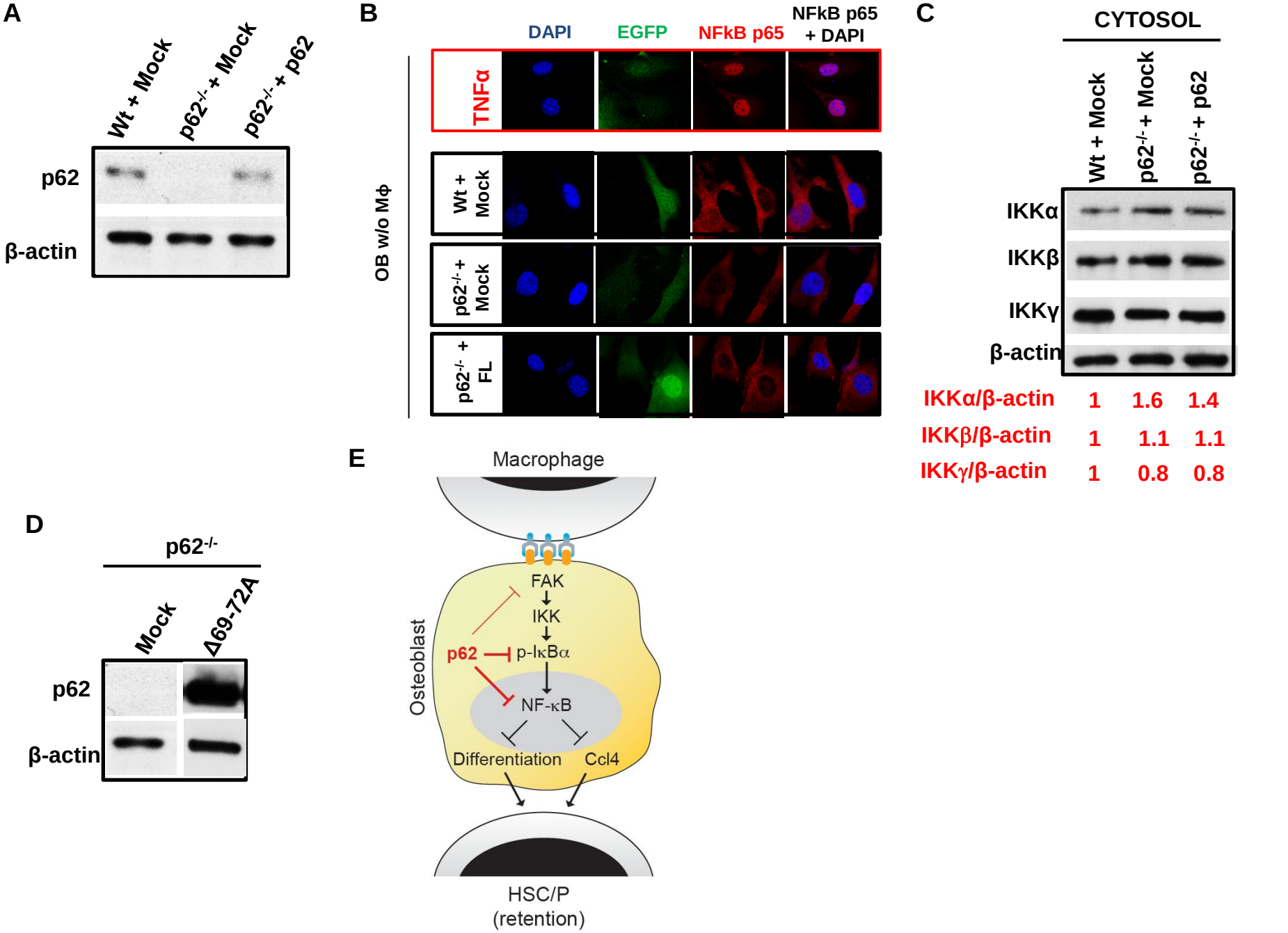
A
Wt + Mock
p62-/- + Mock
p62-/- + p62
p62
β-actin
B
DAPI
EGFP
NFkB p65
NFkB p65 + DAPI
TNFα
OB w/o Mφ
Wt + Mock
p62-/- + Mock
p62-/- + FL
C
CYTOSOL
Wt + Mock
p62-/- + Mock
p62-/- + p62
IKKα
IKKβ
IKKγ
β-actin
IKKα/β-actin 1 1.6 1.4
IKKβ/β-actin 1 1.1 1.1
IKKγ/β-actin 1 0.8 0.8
D
p62-/-
Mock
Δ69-72A
p62
β-actin
E
Macrophage
FAK
IKK
p62
p-IκBα
NF-κB
Differentiation
Ccl4
Osteoblast
HSC/P
(retention)